

UC Davis

UC Davis Previously Published Works

Title

Structural determinants at the M2 muscarinic receptor modulate the RGS4-GIRK response to pilocarpine by impairment of the receptor voltage sensitivity.

Permalink

<https://escholarship.org/uc/item/5s60273q>

Journal

Scientific reports, 7(1)

ISSN

2045-2322

Authors

Chen, I-Shan
Furutani, Kazuharu
Kurachi, Yoshihisa

Publication Date

2017-07-01

DOI

10.1038/s41598-017-05128-z

Peer reviewed

SCIENTIFIC REPORTS

OPEN

Structural determinants at the M2 muscarinic receptor modulate the RGS4-GIRK response to pilocarpine by impairment of the receptor voltage sensitivity

I-Shan Chen¹, Kazuharu Furutani^{1,2} & Yoshihisa Kurachi^{1,2}

Membrane potential controls the response of the M2 muscarinic receptor to its ligands. Membrane hyperpolarization increases response to the full agonist acetylcholine (ACh) while decreasing response to the partial agonist pilocarpine. We previously have demonstrated that the regulator of G-protein signaling (RGS) 4 protein discriminates between the voltage-dependent responses of ACh and pilocarpine; however, the underlying mechanism remains unclear. Here we show that RGS4 is involved in the voltage-dependent behavior of the M2 muscarinic receptor-mediated signaling in response to pilocarpine. Additionally we revealed structural determinants on the M2 muscarinic receptor underlying the voltage-dependent response. By electrophysiological recording in *Xenopus* oocytes expressing M2 muscarinic receptor and G-protein-gated inwardly rectifying K⁺ channels, we quantified voltage-dependent desensitization of pilocarpine-induced current in the presence or absence of RGS4. Hyperpolarization-induced desensitization of the current required for RGS4, also depended on pilocarpine concentration. Mutations of charged residues in the aspartic acid-arginine-tyrosine motif of the M2 muscarinic receptor, but not intracellular loop 3, significantly impaired the voltage-dependence of RGS4 function. Thus, our results demonstrated that voltage-dependence of RGS4 modulation is derived from the M2 muscarinic receptor. These results provide novel insights into how membrane potential impacts G-protein signaling by modulating GPCR communication with downstream effectors.

Membrane potential controls physiological events through regulating a variety of protein functions, including modulation of ligand binding and signal transduction in G-protein-coupled receptors (GPCRs)^{1–5}. The M2 muscarinic receptor is the one of the most intensively studied GPCRs in its voltage-dependent behaviors and molecular mechanisms^{1–4, 6–12}. For example, membrane hyperpolarization increases the affinity of the M2 muscarinic receptor for its native full agonist, acetylcholine (ACh), and decreases affinity for its partial agonist pilocarpine^{3, 9, 10}. Conversely, pilocarpine binding enhances the voltage-induced conformational change of the M2 muscarinic receptor, while ACh binding immobilizes the charge movement⁴. Therefore, access to some conformational states of the M2 muscarinic receptor is thought to be dependent on the binding of specific agonists, and membrane potential modulates the transition between these conformational states^{2, 10, 11, 13}. However, how the voltage-dependent states stabilized by different agonists regulate cellular responses is not well understood.

One of the important regions for the voltage-dependent behavior of M2 muscarinic receptor toward its agonist is intracellular loop 3, which is also the key motif responsible for G-protein interaction^{3, 12, 14, 15}. Mutation of amino acid residues KKDKK located in the N-terminal region of intracellular loop 3 to the sequence ELAAL abolish the voltage-dependence of ACh binding^{3, 12}. The aspartic acid-arginine-tyrosine (DRY) motif of the M2 muscarinic receptor could also be an important region for its voltage-sensitivity³. The DRY motif is critical for regulating GPCR conformational states and agonist-induced response^{6, 14, 16, 17}. Neutralization of D120^{3, 49} and

¹Department of Pharmacology, Graduate School of Medicine, Osaka University, Suita, Osaka, 565-0871, Japan. ²Global Center for Medical Engineering and Informatics, Osaka University, Suita, Osaka, 565-0871, Japan. Correspondence and requests for materials should be addressed to K.F. (email: furutani@pharma2.med.osaka-u.ac.jp) or Y.K. (email: ykurachi@pharma2.med.osaka-u.ac.jp)

R121^{3,50} (D120N/R121N mutant) in the DRY motif has been proposed to abolish the charge movement of the M2 muscarinic receptor³. However, another study concluded that gating current still occurs in the D120N/R121N mutant and therefore these residues are not the key motif responsible for voltage sensor⁴. Therefore, it remains controversial whether the DRY motif acts as a voltage sensor or not^{1,7}. There is also no evidence whether the voltage sensor function of the M2 muscarinic receptor via DRY motif or the intracellular loop 3 can regulate its downstream G-protein signaling regulators.

We previously revealed that the regulator of G-protein signaling (RGS) 4 protein modulates the cellular efficacy of pilocarpine¹⁸. RGS proteins are known to negatively regulate G-protein signaling by accelerating GTP hydrolysis to GDP by G_α subunit and thereby terminating the G-protein signal^{19–23}. Pilocarpine promotes the RGS4-mediated inhibition of M2 muscarinic receptor-activated G-protein signaling, leading to a smaller G-protein-gated inwardly rectifying K⁺ (GIRK) current than that of ACh¹⁸. Importantly, membrane potential controls this phenomenon¹⁸. However, how RGS4 is involved in the voltage-dependent behavior of M2 muscarinic receptor-activated signaling remains unclear.

Since RGS4 is not a membrane protein, RGS4 seems unlikely to function as a voltage sensor. This suggests the voltage sensitivity of RGS4 is derived from its coupled membrane protein, M2 muscarinic receptor. If so, the M2 muscarinic receptor would act as a voltage sensor not only toward its agonists but also toward the RGS4. The DRY motif and the intracellular loop 3 at the M2 muscarinic receptor are candidates for the structural determinants which contribute to the voltage-dependence of RGS4.

Here, we characterized the voltage-dependence of RGS4 modulation on M2 muscarinic receptor-activated signaling and revealed which receptor motif contributes to the underlying mechanism. With electrophysiological recordings from *Xenopus* oocytes, we demonstrate that RGS4 triggers a voltage-dependent current decay of pilocarpine-induced GIRK current. By structure-function analysis of the DRY motif and the intracellular loop 3 of M2 muscarinic receptor using mutagenesis methods, we observed that mutations of charged residues in the DRY motif (D120^{3,49} and R121^{3,50}), instead of intracellular loop 3, significantly impaired the voltage-dependence of RGS4 modulation. The results demonstrate a novel mechanism that membrane potential modulates RGS4 function through the voltage-sensitive M2 muscarinic receptor.

Results

RGS4 modulation of M2 muscarinic receptor-mediated GIRK currents by pilocarpine is voltage-dependent. To understand the effects of membrane potential on RGS4 function, we recorded the M2 muscarinic receptor-activated GIRK currents in rat atrial myocytes and *Xenopus* oocytes heterologously expressing the M2 muscarinic receptor, a cardiac-type GIRK channel (Kir3.1/Kir3.4 heterotetramer²⁴) and RGS4^{25,26}.

In atrial myocytes (Fig. 1a,b) and oocytes expressing RGS4 (Fig. 1c,d), pilocarpine-induced GIRK currents during membrane hyperpolarization reached a peak (I_p) and then decreased to steady state by pulse-end (I_s). This current decay suggests a desensitization of GIRK currents to pilocarpine at hyperpolarized potential in the presence of RGS4. The tau of current decay in the presence of 100 μ M pilocarpine at -140 mV in RGS4-expressing oocytes was 0.47 ± 0.02 s ($n = 6$). This phenomenon was found to be due to the cessation of G-protein activation by modulation of GTP hydrolysis via RGS4 in our previous study using GTP γ S¹⁸, a non-hydrolyzable analog of GTP. The current decay during hyperpolarization was not observed in the absence of RGS4 (Fig. 1e,f), suggesting that RGS4 is a crucial mediator in the hyperpolarization-induced desensitization of the GIRK channel. This suggests that the mechanism of desensitization is an RGS4-mediated reduction in active G-proteins. Note that the term ‘desensitization’ does not imply an insensitivity of the GIRK channel itself.

In oocytes expressing RGS4, with 100 μ M pilocarpine, I_s during -140 mV pulses was smaller than I_p at more positive potentials (Fig. 1c). However, the current-voltage (I-V) curve of I_p was linear at hyperpolarized potentials, indicating GIRK currents are not yet desensitized immediately after hyperpolarization (Fig. 1d). The I-V curve of I_s showed a different shape from that of I_p . The differences in current amplitude between I_p and I_s indicate that desensitization increases as the membrane potential become more hyperpolarized (Fig. 1d). This phenomenon was not observed in the absence of RGS4 (Fig. 1e,f). The results demonstrate that hyperpolarization acts through RGS4 to desensitize GIRK channels to pilocarpine.

We next normalized the GIRK currents induced by different concentrations of pilocarpine with the same amplitude of I_p and then compared the level of I_s in the presence and absence of RGS4 (Fig. 2a,b). With RGS4, we observed that a higher concentration (100 μ M) of pilocarpine had more impact on the normalized I_s level than a lower concentration (1 μ M). The ratio I_s/I_p decreased at high concentrations of pilocarpine and hyperpolarized potentials in the presence of RGS4 (Fig. 2c), suggesting that RGS4 inhibits GIRK currents in a pilocarpine concentration-dependent manner. We then fitted the concentration-response curve of I_s and I_p at -100 mV in the presence of RGS4 with the Hill equation (Fig. 2d). There was no considerable difference in the $-\log EC_{50}$ of I_s and I_p ($-\log EC_{50}$ was 6.23 ± 0.12 M for I_s ; 6.11 ± 0.02 M for I_p), indicating that the receptor affinity of pilocarpine was not substantially changed by the presence of RGS4 modulation. We observed the maximal inhibitory effect of RGS4 modulation in the presence of saturated concentration of pilocarpine (100 μ M). These results suggest that RGS4-GIRK response is voltage-dependent, and this depends on pilocarpine binding to the M2 muscarinic receptor.

Membrane potential rapidly modulates RGS4-mediated desensitization of M2 muscarinic receptor-GIRK signaling.

We next characterized the kinetics of the voltage-dependent response. The time course of GIRK current recovery from desensitization was examined with two hyperpolarizing pulses protocol (-100 mV for 2 s) which were separated by an interpulse (0 mV) of different durations (0.1, 0.3, 0.5, 0.7 and 0.9 s) (Fig. 3). Compared with the first hyperpolarizing pulse in the presence of RGS4, the pilocarpine-induced current showed a smaller I_p at the second hyperpolarizing pulse when the interpulse duration was 0.1 s (Fig. 3a). Prolonging the duration of interpulse to 0.5 s recovered the current amplitude of I_p . The tau of I_p recovery was

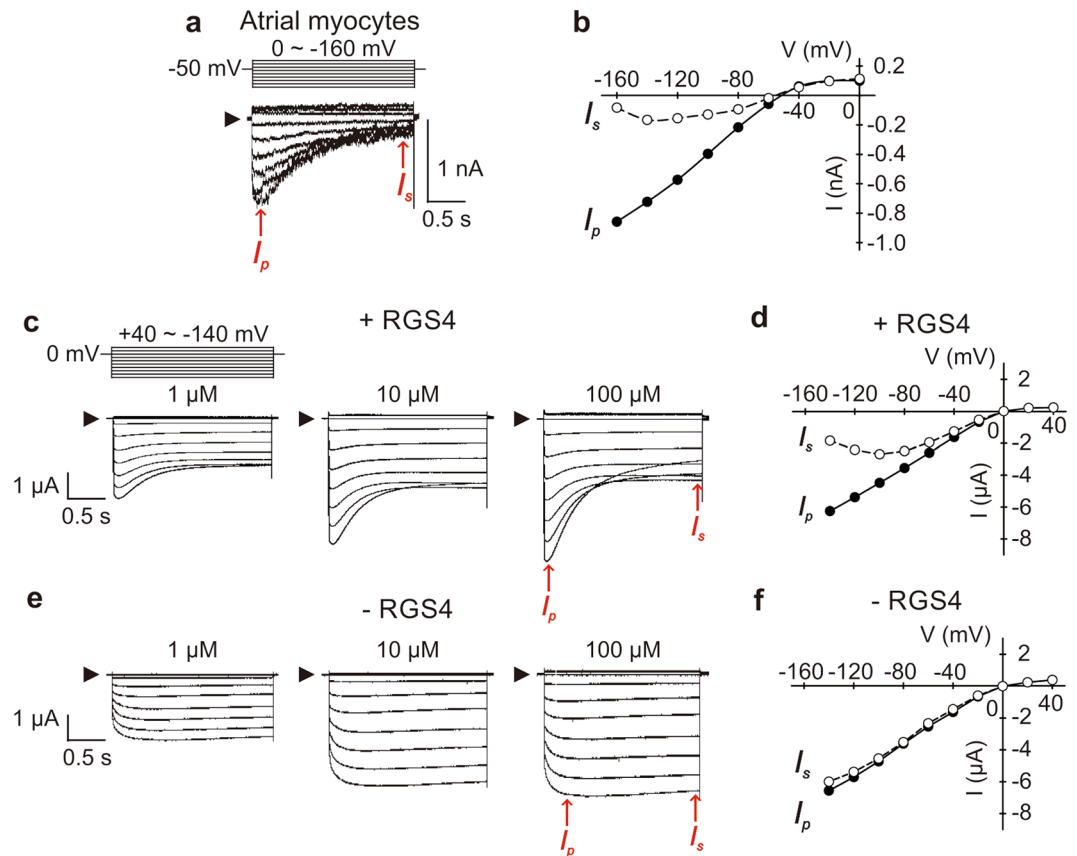


Figure 1. Voltage-dependent response of pilocarpine-induced GIRK currents in rat atrial myocytes and *Xenopus* oocytes. **(a)** Pilocarpine (100 μ M)-induced GIRK currents in rat atrial myocytes were recorded with a step pulse protocol as shown above the current traces. Basal currents were subtracted. **(b)** I-V curve of pilocarpine-induced GIRK currents in atrial myocytes. I_p (filled circles) indicates the peak current at an activated state of GIRK channel; I_s (open circles) indicates the steady-state current at the end of the voltage pulse. Red arrows in **a** were used to reconstruct the I-V curve in **b**. **(c–f)** Pilocarpine (1, 10, 100 μ M)-induced GIRK currents in *Xenopus* oocytes expressing M2 muscarinic receptor, Kir3.1/Kir3.4 with **(c,d)** and without **(e,f)** RGS4 were recorded with a step pulse protocol shown above. Basal currents were subtracted. Amplitudes of I_p and I_s indicated by red arrows in **c** and **e** were used to reconstruct the I-V curve in **d** and **f**.

0.16 ± 0.01 s ($n = 6$) by exponential curve fitting. We did not observe hyperpolarization-induced desensitization in the absence of RGS4 (Fig. 3b). The results demonstrate that the M2 muscarinic receptor-GIRK signaling recovers from hyperpolarization-induced RGS4-mediated desensitization very rapidly.

Mutations in the DRY motif of the M2 muscarinic receptor, instead of intracellular loop3, impaired RGS4 modulation of GIRK current mediated by pilocarpine. To reveal the mechanism which underlies the voltage-dependence of RGS4 modulation, we focused on the voltage-sensitive M2 muscarinic receptor. We examined several charged amino acid residues of the M2 muscarinic receptor which are highly conserved in the rhodopsin-like GPCR family and may act as a voltage-sensor (Fig. 4a).

We first mutated charged residues D69^{2,50} and D103^{3,32} (Fig. 4a,b), are in the transmembrane domains (TMs) of M2 muscarinic receptor and are relevant to voltage sensing and receptor activation^{4, 27, 28}. Consistent with previous studies, we found that mutation of these residues to alanine (D69A and D103A) or asparagine (D69N and D103N) abolished ACh- and pilocarpine-induced GIRK currents in oocytes (Supplementary Fig. S1). This change may be due to the impairment of ligand binding in the mutation of D103^{3,32} or the reduced protein surface expression in the mutation of D69^{2,50}.

We next mutated charged residues D120^{3,49} and R121^{3,50} located in the DRY motif of the M2 muscarinic receptor (Fig. 4a,b). Mutations that neutralized the charges of D120^{3,49} (D120N) or R121^{3,50} (R121N) singly, or both residues together (D120N/R121N), decreased the amplitude difference between the I_p and the I_s of pilocarpine-evoked GIRK currents at -100 mV (Fig. 4d–f), as compared with that of wild-type (WT) M2 muscarinic receptor (Fig. 4c) in the presence of RGS4. During a hyperpolarization pulse, the currents of oocytes expressing these three mutants only showed a modest decrease from I_p to I_s in the presence of RGS4 (Fig. 4d–f, left panel). Such current decay during hyperpolarization was not seen in the absence of RGS4 (Fig. 4c–f, right panel). The ratios I_s/I_p of the M2 muscarinic receptor mutants were significantly elevated compared with WT M2 muscarinic receptor (0.83 ± 0.03 for D120N; 0.91 ± 0.02 for R121N; 0.79 ± 0.01 for D120N/R121N; 0.53 ± 0.04 for WT, $P \leq 0.001$ for each mutant when compared with WT) (Fig. 4g). This suggests that neutralization of

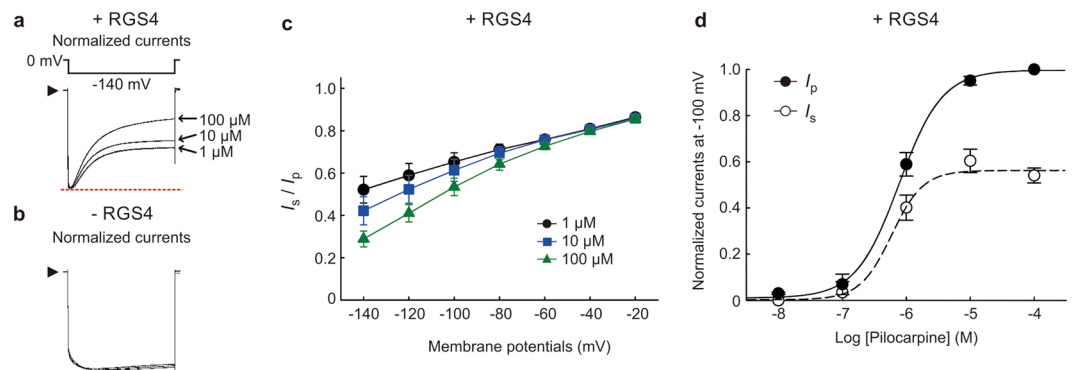


Figure 2. Effects of RGS4 on modulation of GIRK current in a pilocarpine concentration-dependent manner. (a,b) Pilocarpine (1, 10, 100 μ M)-induced GIRK currents in *Xenopus* oocytes expressing M2 muscarinic receptor, Kir3.1/Kir3.4 with (a) and without (b) RGS4 were recorded at -140 mV with the test pulse protocol shown above. The I_p evoked by different concentrations of pilocarpine (1, 10, 100 μ M) were normalized to the same level (red dashed line). Different levels of I_s in the presence of different pilocarpine concentrations were observed. (c) The ratio of I_s to I_p (I_s/I_p) at hyperpolarized potentials (-20 mV to -140 mV) in the applications of pilocarpine (1 μ M, black circles; 10 μ M, blue squares; 100 μ M, green triangles) in oocytes expressing RGS4. Data are means \pm s.e.m., $n = 6-10$. (d) Concentration-response curves of I_s (filled circles) and I_p (open circles) of pilocarpine-induced GIRK current in the presence of RGS4 were fitted with the Hill equation. The maximal value of I_p of pilocarpine-induced GIRK current was normalized to 1. The $-\log EC_{50}$ was 6.23 ± 0.12 M for I_s ; 6.11 ± 0.02 M for I_p . Data are means \pm s.e.m., $n = 3-6$.

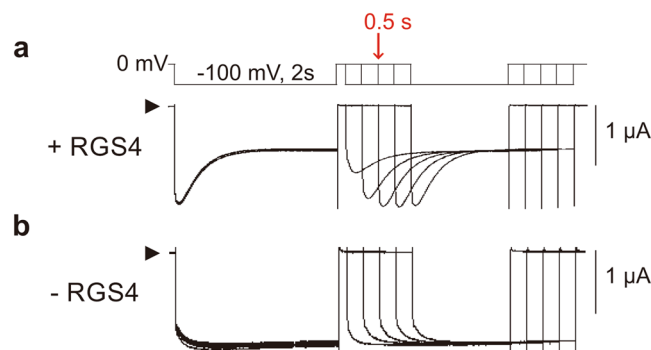


Figure 3. Effects of RGS4 on the recovery of GIRK currents from desensitization. (a,b) Pilocarpine (100 μ M)-induced GIRK currents in oocytes expressing M2 muscarinic receptor, Kir3.1/Kir3.4 with (a) and without (b) RGS4 were recorded with a protocol shown above. Current were recorded with two hyperpolarizing pulses from 0 mV to -100 mV for 2 s which were separated by an interpulse of 0 mV for a duration range of 0.1, 0.3, 0.5, 0.7 and 0.9 s. The fully recovery of GIRK current from the desensitized state can be observed when interpulse (0 mV) duration is longer than 0.5 s. Time constant for the recovery was fitted with exponential curve and discussed in the result section.

D120^{3,49} or R121^{3,50} diminishes the hyperpolarization-induced desensitization of GIRK current by RGS4. To confirm whether mutations of D120^{3,49} and R121^{3,50} affect the pilocarpine-induced current, we calculated the concentration-response curves of these mutants. The concentration-response curves of D120N for pilocarpine (Fig. 4h and Supplementary Fig. S2) and ACh-induced GIRK currents (Supplementary Fig. S3) were similar with WT, while the concentration-response curves of R121N for both pilocarpine and ACh were a rightward shift from that of WT. The 100 μ M concentration of pilocarpine saturated current in all DRY mutants we tested. Although, as we shown in Fig. 2, the pilocarpine-bound M2 muscarinic receptor enhances RGS4-mediated desensitization of GIRK response at hyperpolarized potentials, the DRY motif mutants impaired this function. Therefore, the DRY motif of the M2 muscarinic receptor is an essential structural determinant of the voltage sensitivity of RGS4.

Since the intracellular loop 3 of the M2 muscarinic receptor is also involved in the voltage-dependence of ACh binding³, we examine the roles of the intracellular loop 3 in the voltage-dependence of RGS4 modulation of pilocarpine-induced GIRK current. Interestingly, we found that, in our oocyte expression system, the M2 muscarinic receptor ELAAL mutant retained voltage-dependent response of pilocarpine-induced GIRK currents in the presence of RGS4 (Fig. 5a). The current of ELAAL mutant showed normal hyperpolarization-induced current decay in the presence of RGS4. The I_s/I_p of ELAAL mutant (0.55 ± 0.05 , $n = 6$) was similar to that of WT M2 muscarinic receptor (0.53 ± 0.04 , $n = 6$) (Fig. 5b), suggesting that the N-terminal region of intracellular loop 3 is not essential for the voltage-dependence of RGS4 modulation. The current of ELAAL mutant fully recovered I_p

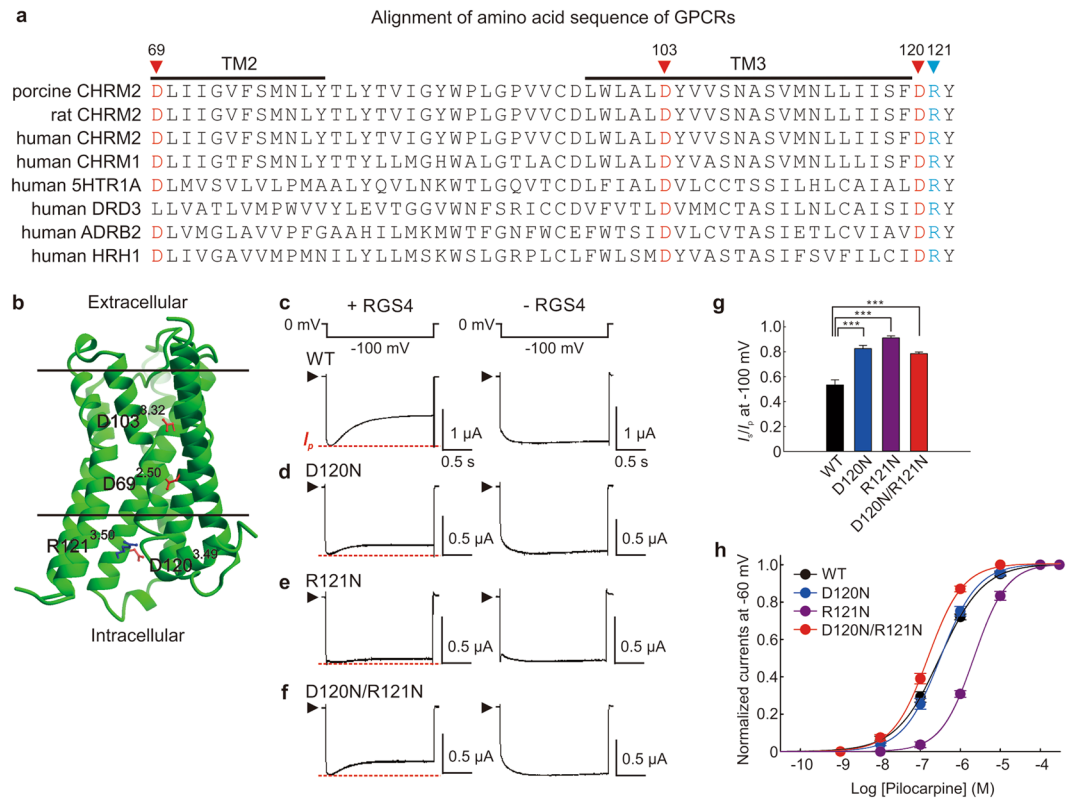


Figure 4. Charged residues in the DRY motif of the M2 muscarinic receptor contribute to the voltage-dependent response of GIRK currents. **(a)** Alignment of amino acids of different species of M2 muscarinic receptors and other human rhodopsin-like GPCRs. Triangles indicate the position of charged residues D69^{2,50}, D103^{3,32}, D120^{3,49} and R121^{3,50}. **(b)** M2 muscarinic receptor model was based on the crystal structure (PDB accession 4MQS)²⁷. The charged residues that we investigated in this study are colored. **(c–f)** Pilocarpine (100 μ M)-induced GIRK currents in oocytes expressing the WT M2 muscarinic receptor **(c)** or mutants D120N **(d)**, R121N **(e)** and D120N/R121N **(f)** with *(left panels)* and without *(right panels)* RGS4 were recorded at -100 mV as shown above. **(g)** The ratio of I_s to I_p (I_s/I_p) of pilocarpine-induced GIRK current at -100 mV in oocytes expressing M2 muscarinic receptor WT and mutants. **(h)** Concentration-response curves of pilocarpine-induced GIRK current were fitted with the Hill equation. The maximal value of pilocarpine-induced GIRK current was normalized to 1. The $-\log EC_{50}$ was 6.51 ± 0.01 for WT; 6.81 ± 0.01 for D120N; 5.66 ± 0.01 for R121N; 6.50 ± 0.01 for D120N/R121N. Data in **g** and **h** are means \pm s.e.m., $n = 6–8$. ***Indicates a statistically significant difference ($P \leq 0.001$).

from the desensitization when the interpulse duration was 0.9 s, longer than with the WT M2 muscarinic receptor (Fig. 5c). The tau for I_p recovery was 0.16 ± 0.01 s for WT and 0.34 ± 0.01 s for ELAAL, respectively ($n = 6$ for each, $P < 0.001$ in Fig. 5d). The slow I_p recovery of ELAAL mutant from the hyperpolarization-induced desensitization suggests that this mutant takes a longer time to recover the GIRK current from RGS4 modulation as compared with WT. The I_s/I_p was, however, not influenced by mutation of KKDKK to ELAAL (Fig. 5b). Concentration-response curves of ELAAL mutant for pilocarpine (Fig. 5e and Supplementary Fig. S2) and ACh (Supplementary Fig. S3) were slightly rightward shifted as compared with that of WT. Taken together, the results indicate that the N-terminal region of intracellular loop 3 is not essential for voltage-dependence of RGS4.

Discussion

In the present study, we find that membrane potential modulates RGS4 function through the voltage-sensitive M2 muscarinic receptor. Hyperpolarization enhanced the RGS4-mediated inhibition of pilocarpine-induced GIRK currents in both rat atrial myocytes and *Xenopus* oocytes (Fig. 1). This phenomenon is dependent on the pilocarpine concentration (Figs 1 and 2). A previous study suggested that hyperpolarization induces a decrease in M2 muscarinic receptor affinity toward pilocarpine in cat atrial myocytes⁹. However, in the absence of RGS4, pilocarpine-induced GIRK current only showed a negligible decrease in current amplitude during hyperpolarization. Therefore, the hyperpolarization-induced desensitization of GIRK channel appears to be due to the increase in the capability of RGS4 modulation, not a decrease in ligand affinity.

Analyses of gating charge-movement and reporter fluorescent signal associated with M2 muscarinic receptor have suggested that a voltage-induced conformational change in M2 muscarinic receptor occurs very rapidly, within 0.01 s^{3,4,12}. This would precede the voltage-induced changes in RGS4 function. Our results showed that RGS4-mediated desensitization of GIRK currents recovers rapidly (tau of recovery time was about 0.16 s) at

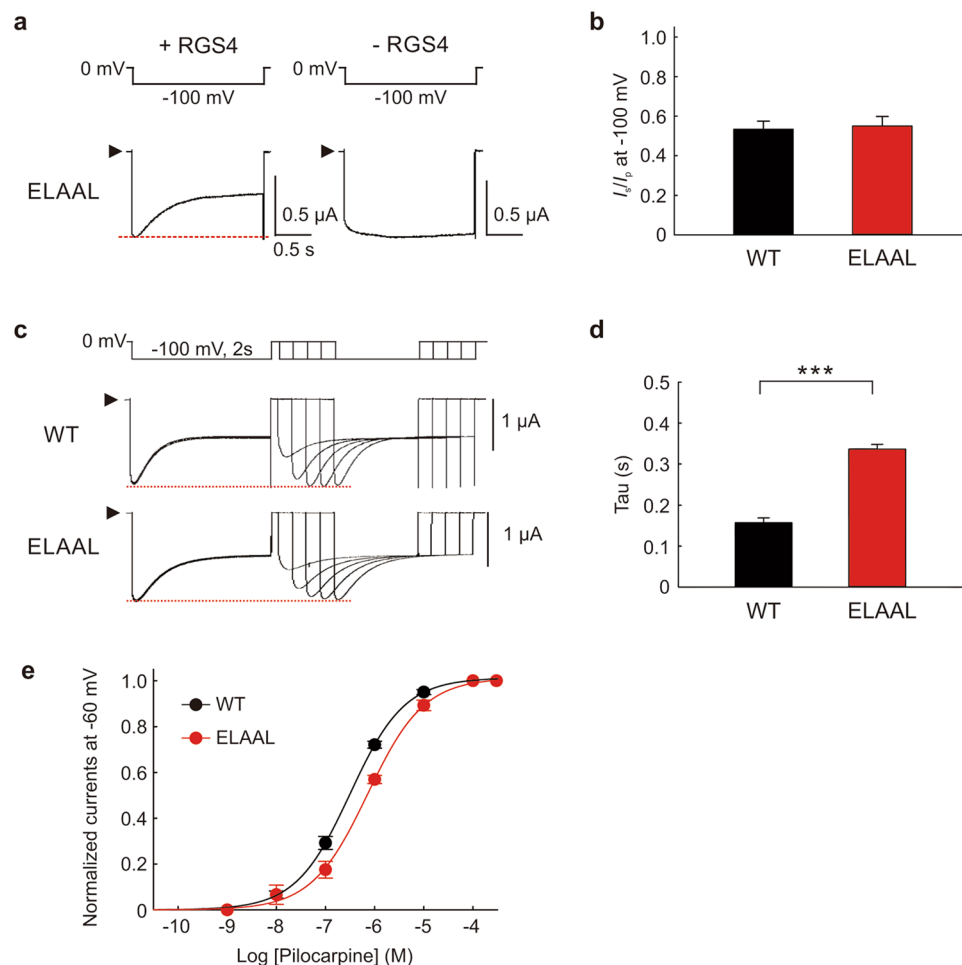


Figure 5. Effects of mutations in the intracellular loop 3 of M2 muscarinic receptor on the voltage-dependent response of GIRK currents. **(a)** Pilocarpine (100 μ M)-induced GIRK currents in oocytes expressing M2 muscarinic receptor mutant ELAAL with (left panels) and without (right panels) RGS4 were recorded at -100 mV as shown above. **(b)** The ratio of I_s to I_p (I_s/I_p) of M2 muscarinic receptor WT and ELAAL at -100 mV in the presence of pilocarpine (100 μ M). **(c)** Recoveries of pilocarpine (100 μ M)-induced GIRK currents from hyperpolarization-mediated desensitization of channels in oocytes expressing WT and ELAAL M2 muscarinic receptors were recorded with a protocol shown above the current traces. **(d)** The time constant (τ) of I_p recovery times in **c** were calculated with exponential curve fitting. **(e)** Concentration-response curves of pilocarpine-induced GIRK currents were fitted with the Hill equation. The maximal value of pilocarpine-induced GIRK current was normalized to 1. The $-\log EC_{50}$ was 6.51 ± 0.02 for WT; 6.15 ± 0.02 for ELAAL. Data in **b**, **d** and **e** are means \pm s.e.m., $n = 6$. ***Indicates a statistically significant difference ($P < 0.001$).

holding membrane potential (Fig. 3), and this event would follow the receptor conformational change mediated by voltage change.

We showed that D120^{3.49} or R121^{3.50} in the DRY motif of M2 muscarinic receptor contribute to the voltage-dependence of RGS4 modulation of GIRK current. These charged residues are part of the underlying mechanism that enhances the capability of RGS4 modulation at hyperpolarized potentials (Fig. 4). This result indicates that the voltage-dependence of RGS4 is derived from the M2 muscarinic receptor. One possible mode of action for D120^{3.49} and R121^{3.50} is that these residues act as part of voltage sensors in the receptor for sensing membrane potential. Another possible mode is that these residues are required for its interaction with RGS4 because DRY motif is located on the cytosolic side of the plasma membrane. However, it is most likely that these charged residues support the pathway that mediates voltage-dependent conformational change of the M2 muscarinic receptor because these charged residues form a part of charge-charge interaction which stabilizes the receptor conformation¹⁴. These charged residues respectively interact with other residues located in the TM2 and TM6 as well^{14, 16, 27}. Once the negative charge of D120^{3.49} is neutralized, the converse R121^{3.50} is probably free to move to find another ionic partner²⁹ and vice versa. Therefore, neutralization of both D120^{3.49} and R121^{3.50} or only one of them disturbs the balance of charge-charge interaction within receptor and thus altering the voltage-sensitivity.

Other charged residues of the M2 muscarinic receptor are relevant to the voltage sensing, including D69^{2.50} and D103^{3.32}. However, mutations of D69^{2.50} or D103^{3.32} appear to reduce both receptor expression and agonist

binding^{4, 27, 28}. These changes may be the reason why we could not observe agonist-induced currents and limits our evaluation of their roles to the present experimental design.

Membrane potential regulates the binding and dissociation of ACh with the M2 muscarinic receptor through the N-terminal region of the intracellular loop 3^{31, 12, 30}. In the present study, we showed that replacing the N-terminal region of the intracellular loop 3 of the M2 muscarinic receptor (residues KKDKK) to ELAAL decelerates the recovery of the voltage-induced change in pilocarpine-induced GIRK current as compared with WT in the presence of RGS4 (Fig. 5). Several studies have demonstrated that replacing intracellular loop 3 of the M2 muscarinic receptor with the corresponding sequence from the M1 muscarinic receptor or β_1 -adrenergic receptor changes the specificity for different subtypes of G_α and changes the ligand-mediated activation of G-protein signaling^{31–33}. Therefore, the affinity of the ELAAL mutant for the $G_{i/o}$ type of G_α should be different from WT M2 muscarinic receptor. The $G_{i/o}$ -RGS4 complex may be associated with intracellular loop 3 of the ELAAL mutant in a less stable state, as compared with WT, and thus decelerates the recovery of G-protein signaling from RGS4-mediated regulation.

Recent studies demonstrated that the voltage-dependence of the M1 muscarinic receptor toward ACh binding is opposite to the M2 muscarinic receptor² and replacing intracellular loop 3 of the M2 muscarinic receptor with that of M1 muscarinic receptor gives the mutated receptor the voltage-dependence of the M1 muscarinic receptor³. However, our results demonstrated that the ELAAL mutant retains the voltage-dependence of RGS4 function. This suggests that this region is responsible for the voltage-regulated coupling of the GPCR to its G-protein³⁰, and this pathway is independent to the voltage-dependence of RGS4 modulation on G-protein signal. Taken together, both the positive pathway (agonist-induced activation) and the negative pathway (RGS4-mediated inhibition) of G-protein signaling are controlled by voltage via different motif at M2 muscarinic receptor, and thus modulating the receptor communication with downstream effectors, $G_{i/o}$ and RGS4.

As several RGS-associated GPCRs have been identified^{34–37}, further research will be required to fully understand the interaction between the receptor and RGS protein, which underlies the voltage-dependent modulation of RGS in regulating downstream GPCR signaling. The C-terminal tail of GPCR proteins is a candidate region for mediating the association between RGS proteins and GPCRs^{38, 39}.

In the present study, we showed that membrane potential modulates RGS4 function through the voltage-sensitive M2 muscarinic receptor. Especially at hyperpolarized potentials, pilocarpine, which categorized as a “partial agonist” may, in fact, stabilize a receptor conformation which leads to relatively high GTP hydrolysis activity as compared to that of a full agonist. This study sheds light on the multimodal functions of the M2 muscarinic receptor in both signal perception and transduction.

Methods

Animals and cell preparations. Animal experiments were performed in accordance with the guidelines for the use of laboratory animals of Osaka University Graduate School of Medicine. The experimental protocol was approved by the Institutional Animal Care and Use Committee and the Animal Experiments Committee of Osaka University. Single atrial myocytes were enzymatically isolated from hearts of adult male Wistar rats (200–300 g) as previously described⁴⁰ and maintained in KB solution containing 10 mM taurine, 10 mM oxalic acid, 70 mM glutamic acid, 25 mM KCl, 10 mM KH_2PO_4 , 0.5 mM EGTA, 11 mM glucose and 10 mM HEPES (pH 7.3 with KOH, 295–300 mOsm L^{-1}). Freshly isolated cells were used in patch clamp experiments on the day.

The cRNA of porcine M2 muscarinic receptor (80 ng oocyte⁻¹), mouse Kir3.1 (8 ng oocyte⁻¹), rat Kir3.4 (8 ng oocyte⁻¹) and rat RGS4 (160 ng oocyte⁻¹) were used in this study. The porcine M2 muscarinic receptor was encoded on pSP64T plasmid. Point mutations in the M2 muscarinic receptor were constructed by PCR mutagenesis and verified by sequencing. The positions of amino acid residues of M2 muscarinic receptor are indicated by their generic number according to the Ballesteros–Weinstein nomenclature⁴¹. Complementary RNAs were transcribed from the cDNA by mMessage mMachine kit (Ambion). *Xenopus laevis* oocytes were prepared and injected with cRNA as described previously⁴². After injection, oocytes were incubated at 18 °C in ND96 solution containing 96 mM NaCl, 2 mM KCl, 1.8 mM CaCl_2 , 1 mM MgCl_2 and 5 mM HEPES (pH 7.6 with NaOH) and supplemented with gentamicin (50 $\mu\text{g ml}^{-1}$). Currents were recorded 3–5 days after the cRNA injection.

Electrophysiological recording. Voltage-clamped currents of atrial myocytes were recorded in the whole-cell configuration by a patch-clamp amplifier (EPC10, HEKA Electronics, Lambrecht, Germany) at room temperature. Data were low-pass-filtered at 1 kHz (–3 dB) by an eight-pole Bessel filter, sampled at 5 kHz, and analyzed offline with PatchMaster (HEKA Electronics) and FitMaster (HEKA Electronics). Myocytes were recorded in a bath solution containing 115 mM NaCl, 20 mM KCl, 1.8 mM CaCl_2 , 0.53 mM MgCl_2 , 5.5 mM glucose and 5.5 mM HEPES (pH 7.4 with NaOH). The tip resistance of glass electrodes was 2–5 M Ω when filled with the pipette solution containing 150 mM KCl, 5 mM EGTA, 1 mM MgCl_2 , 3 mM K_2ATP , 0.1 mM Na_2GTP and 5 mM HEPES (pH 7.3 with KOH).

For oocytes, membrane currents were recorded using the two-electrode voltage clamp by a GeneClamp 500 amplifier (Molecular Devices, Sunnyvale, CA, USA) at room temperature. Data were reproduced and analyzed with pCLAMP 10 (Molecular Devices) and Clampfit 10.2 (Molecular Devices). The bath solution contained: 90 mM KCl, 3 mM MgCl_2 , 0.15 mM niflumic acid and 5 mM HEPES (pH 7.4 with KOH). The tip resistance of glass electrodes was 0.4–1.5 M Ω when filled with the 3 M KCl pipette solution. Pilocarpine (0.001–300 μM)-induced currents and ACh (0.0001–10 μM)-induced currents were obtained by digitally subtracting the basal currents. The concentration-response curve were measured by sequential application of pilocarpine and ACh in bath solution for 30–60 s at each concentration when current amplitude reached a stable level as shown in Supplementary Figs S2 and S3. 100 μM Pilocarpine-induced current could be washed out within 1–2 min. Concentration-response curve were fitted by Hill equation with SigmaPlot 12 (Hulinks).

Data statistics. Data statistical analysis was performed with SigmaPlot 12 (Hulinks). Results are shown as mean \pm s.e.m. from n cells. Statistical differences between each group were evaluated by Tukey's test. Values of $P < 0.05$ were judged statistically significant. *, ** and *** indicate values of $P < 0.05$, 0.01 and 0.001, respectively.

References

- Vickery, O. N., Machtens, J. P. & Zachariae, U. Membrane potentials regulating GPCRs: insights from experiments and molecular dynamics simulations. *Curr Opin Pharmacol.* **30**, 44–50 (2016).
- Ben-Chaim, Y., Tour, O., Dascal, N., Parnas, I. & Parnas, H. The M2 muscarinic G-protein-coupled receptor is voltage-sensitive. *J Biol Chem.* **278**, 22482–22491 (2003).
- Ben-Chaim, Y. *et al.* Movement of 'gating charge' is coupled to ligand binding in a G-protein-coupled receptor. *Nature.* **444**, 106–109 (2006).
- Navarro-Polanco, R. A. *et al.* Conformational changes in the M2 muscarinic receptor induced by membrane voltage and agonist binding. *J Physiol.* **589**, 1741–1753 (2011).
- Vickery, O. N., Machtens, J. P., Tamburrino, G., Seeliger, D. & Zachariae, U. Structural Mechanisms of Voltage Sensing in G Protein-Coupled Receptors. *Structure.* **24**, 997–1007 (2016).
- Mahaut-Smith, M. P., Martinez-Pinna, J. & Gurung, I. S. A role for membrane potential in regulating GPCRs? *Trends Pharmacol Sci.* **29**, 421–429 (2008).
- Tamuleviciute, A. & Brookfield, R. Muscarinic receptors: electrifying new insights. *J Physiol.* **589**, 4411–4412 (2011).
- Barchad-Avitzur, O. *et al.* A Novel Voltage Sensor in the Orthosteric Binding Site of the M2 Muscarinic Receptor. *Biophys J.* **111**, 1396–1408 (2016).
- Moreno-Galindo, E. G. *et al.* Relaxation gating of the acetylcholine-activated inward rectifier K^+ current is mediated by intrinsic voltage sensitivity of the muscarinic receptor. *J Physiol.* **589**, 1755–1767 (2011).
- Moreno-Galindo, E. G., Alamilla, J., Sanchez-Chapula, J. A., Tristani-Firouzi, M. & Navarro-Polanco, R. A. The agonist-specific voltage dependence of M2 muscarinic receptors modulates the deactivation of the acetylcholine-gated $K(+)$ current (I KACH). *Pflugers Arch.* **468**, 1207–1214 (2016).
- Zohar, A., Dekel, N., Rubinsky, B. & Parnas, H. New mechanism for voltage induced charge movement revealed in GPCRs-theory and experiments. *PLoS One.* **5**, e8752 (2010).
- Dekel, N., Priest, M. F., Parnas, H., Parnas, I. & Bezanilla, F. Depolarization induces a conformational change in the binding site region of the M2 muscarinic receptor. *Proc Natl Acad Sci USA.* **109**, 285–290 (2012).
- Seifert, R., Wenzel-Seifert, K., Gether, U. & Kobilka, B. K. Functional differences between full and partial agonists: evidence for ligand-specific receptor conformations. *J Pharmacol Exp Ther.* **297**, 1218–1226 (2001).
- Haga, K. *et al.* Structure of the human M2 muscarinic acetylcholine receptor bound to an antagonist. *Nature.* **482**, 547–551 (2012).
- Liu, J., Blin, N., Conklin, B. R. & Wess, J. Molecular mechanisms involved in muscarinic acetylcholine receptor-mediated G protein activation studied by insertion mutagenesis. *J Biol Chem.* **271**, 6172–6178 (1996).
- Rovati, G. E., Capra, V. & Neubig, R. R. The highly conserved DRY motif of class A G protein-coupled receptors: beyond the ground state. *Mol Pharmacol.* **71**, 959–964 (2007).
- Greasley, P. J., Fanelli, F., Rossier, O., Abuin, L. & Cotecchia, S. Mutagenesis and modelling of the $\alpha(1b)$ -adrenergic receptor highlight the role of the helix 3/helix 6 interface in receptor activation. *Mol Pharmacol.* **61**, 1025–1032 (2002).
- Chen, I. S., Furutani, K., Inanobe, A. & Kurachi, Y. RGS4 regulates partial agonism of the M2 muscarinic receptor-activated K^+ currents. *J Physiol.* **592**, 1237–1248 (2014).
- Ross, E. M. & Wilkie, T. M. GTPase-activating proteins for heterotrimeric G proteins: regulators of G protein signaling (RGS) and RGS-like proteins. *Annu Rev Biochem.* **69**, 795–827 (2000).
- Koelle, M. R. A new family of G-protein regulators - the RGS proteins. *Curr Opin Cell Biol.* **9**, 143–147 (1997).
- Dohlman, H. G. & Thorner, J. RGS proteins and signaling by heterotrimeric G proteins. *J Biol Chem.* **272**, 3871–3874 (1997).
- Fujita, S., Inanobe, A., Chachin, M., Aizawa, Y. & Kurachi, Y. A regulator of G protein signalling (RGS) protein confers agonist-dependent relaxation gating to a G protein-gated K^+ channel. *J Physiol.* **526**(Pt 2), 341–347 (2000).
- Hepler, J. R. Emerging roles for RGS proteins in cell signalling. *Trends Pharmacol Sci.* **20**, 376–382 (1999).
- Krapivinsky, G. *et al.* The G-protein-gated atrial K^+ channel IKACH is a heteromultimer of two inwardly rectifying $K(+)$ -channel proteins. *Nature.* **374**, 135–141 (1995).
- Zhang, S. *et al.* RGS3 and RGS4 are GTPase activating proteins in the heart. *J Mol Cell Cardiol.* **30**, 269–276 (1998).
- Tomirisa, P., Blumer, K. J. & Muslin, A. J. RGS4 inhibits G-protein signaling in cardiomyocytes. *Circulation.* **99**, 441–447 (1999).
- Kruse, A. C. *et al.* Activation and allosteric modulation of a muscarinic acetylcholine receptor. *Nature.* **504**, 101–106 (2013).
- Furukawa, H. *et al.* Conformation of ligands bound to the muscarinic acetylcholine receptor. *Mol Pharmacol.* **62**, 778–787 (2002).
- Ballesteros, J. *et al.* Functional microdomains in G-protein-coupled receptors. The conserved arginine-cage motif in the gonadotropin-releasing hormone receptor. *J Biol Chem.* **273**, 10445–10453 (1998).
- Ben Chaim, Y., Bochnik, S., Parnas, I. & Parnas, H. Voltage affects the dissociation rate constant of the m2 muscarinic receptor. *PLoS One.* **8**, e74354 (2013).
- Lai, J. *et al.* Chimeric M1/M2 muscarinic receptors: correlation of ligand selectivity and functional coupling with structural modifications. *J Pharmacol Exp Ther.* **262**, 173–180 (1992).
- Wong, S. K. & Ross, E. M. Chimeric muscarinic cholinergic:beta-adrenergic receptors that are functionally promiscuous among G proteins. *J Biol Chem.* **269**, 18968–18976 (1994).
- Wong, S. K. G protein selectivity is regulated by multiple intracellular regions of GPCRs. *Neurosignals.* **12**, 1–12 (2003).
- Croft, W. *et al.* A Physiologically Required GPCR - RGS Interaction that Compartmentalizes RGS Activity. *J Biol Chem.* (2013).
- Hague, C. *et al.* Selective inhibition of $\alpha 1A$ -adrenergic receptor signaling by RGS2 association with the receptor third intracellular loop. *J Biol Chem.* **280**, 27289–27295 (2005).
- Bernstein, L. S. *et al.* RGS2 binds directly and selectively to the M1 muscarinic acetylcholine receptor third intracellular loop to modulate Gq/11 α signaling. *J Biol Chem.* **279**, 21248–21256 (2004).
- Abramow-Newerly, M., Roy, A. A., Nunn, C. & Chidiac, P. RGS proteins have a signalling complex: interactions between RGS proteins and GPCRs, effectors, and auxiliary proteins. *Cell Signal.* **18**, 579–591 (2006).
- Neubig, R. R. & Siderovski, D. R. Regulators of G-protein signalling as new central nervous system drug targets. *Nature Reviews Drug Discovery.* **1**, 187–197 (2002).
- Shukla, A. K., Xiao, K. & Lefkowitz, R. J. Emerging paradigms of beta-arrestin-dependent seven transmembrane receptor signaling. *Trends Biochem Sci.* **36**, 457–469 (2011).
- Ishii, M. *et al.* Ca^{2+} elevation evoked by membrane depolarization regulates G protein cycle via RGS proteins in the heart. *Circ Res.* **89**, 1045–1050 (2001).
- Ballesteros, J. A. & Weinstein, H. Integrated methods for the construction of three-dimensional models and computational probing of structure-function relations in G protein-coupled receptors. *Methods Neurosci.* **25**, 366–428 (1995).
- Inanobe, A. *et al.* Interaction between the RGS domain of RGS4 with G protein α subunits mediates the voltage-dependent relaxation of the G protein-gated potassium channel. *J Physiol.* **535**, 133–143 (2001).

Acknowledgements

We are grateful to Dr. Jon Sack (University of California, Davis, USA) for critical reading of this manuscript. This study was supported by the Hiroshi and Aya Irisawa Memorial Promotion Award for Young Physiologists (to K.F.) from the Physiological Society of Japan, Grants-in-Aid for the Scientific Research on Innovative Areas 22136002 (to Y.K.), 15H01404 (to K.F.), and the Scientific Research (C) 15K08231 (to K.F.) and from the Ministry of Education, Science, Sports and Culture of Japan, and the Japan Society for the Promotion of Science.

Author Contributions

I.-S.C. performed the experiments, analyzed the data and wrote the manuscript. I.-S.C., K.F. and Y.K. designed the study, interpreted the results and revised the manuscript. All authors approved the manuscript.

Additional Information

Supplementary information accompanies this paper at doi:[10.1038/s41598-017-05128-z](https://doi.org/10.1038/s41598-017-05128-z)

Competing Interests: The authors declare that they have no competing interests.

Publisher's note: Springer Nature remains neutral with regard to jurisdictional claims in published maps and institutional affiliations.



Open Access This article is licensed under a Creative Commons Attribution 4.0 International License, which permits use, sharing, adaptation, distribution and reproduction in any medium or format, as long as you give appropriate credit to the original author(s) and the source, provide a link to the Creative Commons license, and indicate if changes were made. The images or other third party material in this article are included in the article's Creative Commons license, unless indicated otherwise in a credit line to the material. If material is not included in the article's Creative Commons license and your intended use is not permitted by statutory regulation or exceeds the permitted use, you will need to obtain permission directly from the copyright holder. To view a copy of this license, visit <http://creativecommons.org/licenses/by/4.0/>.

© The Author(s) 2017